

Highly ordered mesoporous functionalized pyridinium protic ionic liquids framework as efficient system in esterification reactions for biofuels production

Fatemeh Rajabi^{a,*}, Rafael Luque^{b,c}

^a Department of Science, Payame Noor University, P. O. Box: 19395-4697, Tehran 19569, Iran

^b Departamento de Química Orgánica, Universidad de Córdoba, Campus de Rabanales, Edificio Marie Curie (C-3), Ctra Nnal IV-A, Km 396, Córdoba 14014, Spain

^c Peoples Friendship University of Russia (RUDN University), 6 Miklukho Maklaya St., 117198, Moscow, Russia

ARTICLE INFO

To the memory of Prof. Mohammad Reza Saidi, colleague and inspiration for this work, who passed away in 2020.

Keywords:

Nanomaterial
Pyridinium
Protic ionic liquids
Biodiesel
Free fatty acid
PMO
Esterification

ABSTRACT

Polysiloxane acidic ionic liquids containing pyridinium trifluoroacetate salts (PMO-Py-IL) were synthesized from pyridine containing organosilane precursors. Characterization by SEM, XRD, TGA, and nitrogen porosimetry confirmed that both pyridinium cation and trifluoroacetate anion were successfully incorporated within the organosilica network. The resulting organic-inorganic hybrid nanomaterial (PMO-Py-IL) was studied as nano-catalyst in free fatty acids esterification into biodiesel-like compounds. Remarkably, the synergistic hydrophilic/hydrophobic effect of pyridinium and trifluoroacetate ionic liquid in the well-ordered channels of PMO-Py-IL nanomaterial enhanced the activity toward sustainable biodiesel-like esters production. More importantly, PMO-Py-IL nanocatalyst also exhibited an exceptional activity and stability. The catalyst could be easily separated to reuse at least in ten reactions runs preserving almost intact its catalytic activity under otherwise identical conditions to those employed for the fresh catalysts.

1. Introduction

Global awareness of energy and environmental issues related to the burning of non-renewable fuels including petrol oil, natural gas and coal inspired scientists to explore the use of sustainable alternative feedstocks for renewable energy including biofuels [1]. Among renewable biofuel resources, biodiesel comprises long-chain fatty acid esters produced from biomass-derived oils and fats [2–4]. Conventional production of biodiesel is base-catalyzed transesterification of triglycerides contained in oils or fats with methanol or ethanol [5,6]. Despite its utility, soap formation of free fatty acids content in oil feedstock results in low biodiesel yield and difficulty in its separation from glycerol. Esterification of free fatty acids accounts for a promising alternative for the production of biodiesel-like biofuels [7,8]. The well-known synthesis method for ester products, Fischer esterification, as atom economy favors the reaction between carboxylic acids and alcohols for the preparation of esters [9]. Esterification reactions are rather slow in the absence of catalysts, requiring harsh conditions to reach equilibrium. Homogeneous mineral acid catalysts (i.e., H₂SO₄, HCl or H₃PO₄) exhibit

several issues including product separation, installation corrosion and undesired waste production. Therefore, improved catalytic systems with operational simplicity and economic viability are essential for the green and sustainable preparation of target chemical products. Immobilization of homogeneous catalysts with easy handling and possible recyclability can circumvent current issues, providing more sustainable catalyst alternatives. A wide variety of porous supported acid and base catalysts with various organic and inorganic supports including polymers, mesoporous materials and zeolites have been utilized in esterification reactions [10–25]. Several supported catalysts have shown promising catalytic performance in the esterification reaction with an effective separation step. However, the majority exhibited temperature-dependent activities, thus poor recyclability. The weak catalyst support interaction caused catalytic site leaching from the support surface at elevated temperatures.

Hence, highly efficient solid acid catalysts with higher catalytic stability and activity, tunable acidity and surface polarity for sustainable biofuels production are needed.

The use of suitable supports is the most effective approach to

* Corresponding author.

E-mail addresses: f.rajabi@pnu.ac.ir (F. Rajabi), q62alsor@uco.es (R. Luque).

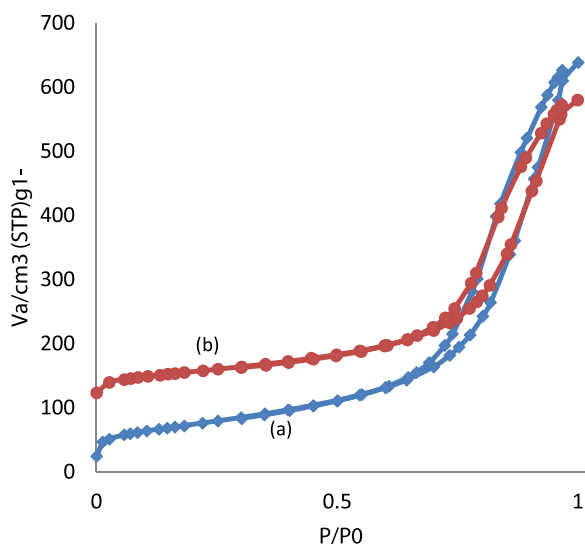


Fig. 1. N₂ physisorption isotherms of a) PMO-Py and b) PMO-Py-IL.

Table 1

Nitrogen adsorption data for PMO-Py and PMO-Py-IL.

Material	Surface Area (m ² g ⁻¹)	Pore Volume (cm ³ g ⁻¹)	Pore diameter (nm)
PMO-Py	610	0.69	6.9
PMO-Py-IL	514	0.61	6.1

overcome these drawbacks. Among solid supports, periodic mesoporous organosilicas (PMOs) with various bridge organo bis-silan are promising in the development of functionally advanced materials. This generation of well-ordered mesoporous materials combines a stable inorganic support together with the presence of homogeneously distributed organic moieties, leading to hybrid organic-inorganic frameworks. Due to excellent characteristics and properties including tunable surface properties, high surface areas and pore sizes, high thermal stabilities, appropriate hydrophobicity and the potential to incorporate a range of organic functionalities into their walls, PMOs have been proved to be excellent systems with a broad variety of potential applications in physics, chemistry, engineering, medicine, biology, and advanced material science [26–34].

Ionic liquids (ILs), a class of low-melting organic salts, have attracted considerable attention as green media and promising catalysts in science

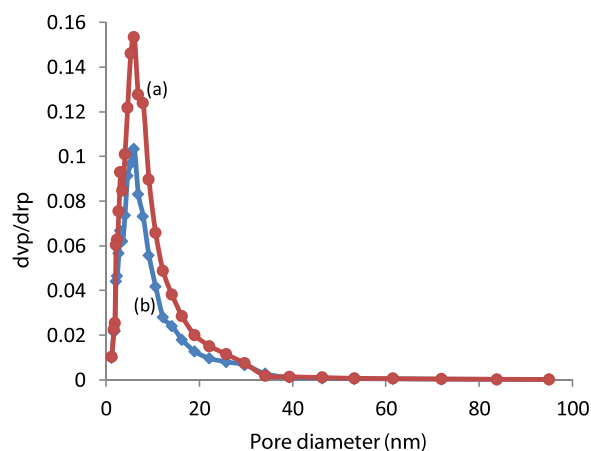


Fig. 2. Pore size distribution (BJH) of a) PMO-Py and b) PMO-Py-IL.

and technology [34–38]. The unique physical and chemical properties of ILs can be tuned by altering nature, size and shape of anions and cations. A sub-class of ILs are protic ionic liquids (PILs), prepared via proton transfer between a Brønsted acid and base. Their ease of preparation and functionalization make them particularly beneficial in thermo-electromechanical devices, gas absorption and separation, organic and inorganic synthesis, biological applications, fuel cells and chromatography. PILs have gained significant attention as acid catalysts in various chemical reactions [39–43]. However, recyclability and separation of PILs from the reaction media is a time and energy consuming process. An alternative is the heterogenization of PILs on solid supports using several approaches such as grafting, impregnation, polymerization, and anchoring. Compared to the considerable research efforts on homogeneous PILs, there is so far little research on supported PILs, despite their obvious importance in green and sustainable chemical process [44–50]. Nevertheless, several challenges such as low catalyst activity, high catalyst amount, poor recyclability and harsh operating conditions remain un-addressed. This work is aimed to develop a stable and reusable supported solid catalyst with high catalytic performance through the simple combination of trifluoroacetic acid and pyridine-based PMO materials. Following previous studies on the preparation of supported catalytic systems for organic transformations [51–53], a porous hydrophobic PMO nanomaterial based on pyridinium ionic liquid organosilica was synthesized and employed as a highly stable and efficient system for the esterification of various free fatty acids and methanol under mild conditions.

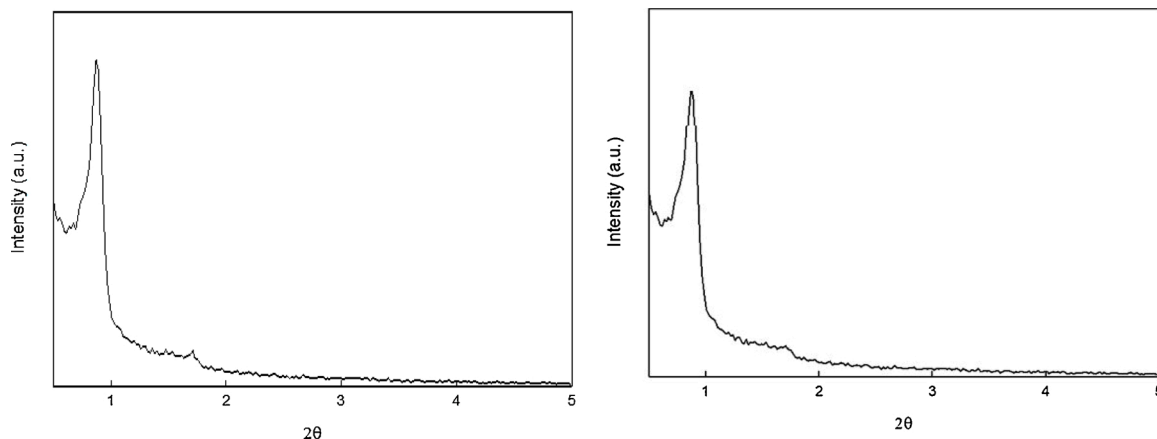


Fig. 3. XRD patterns corresponding to the PMO-Py (left) and PMO-Py-IL (right).

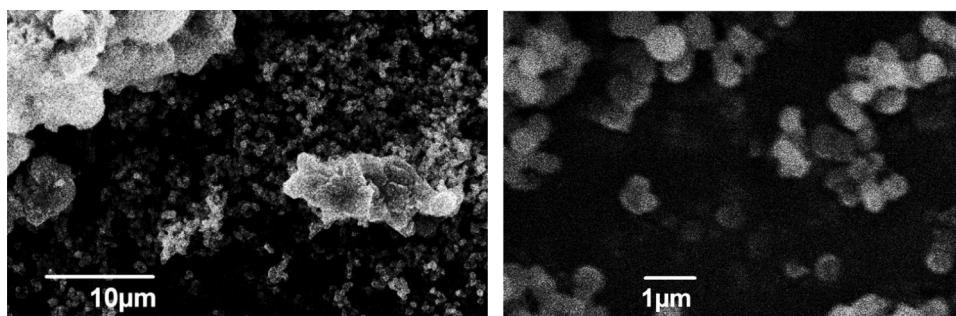


Fig. 4. SEM images of PMO-Py-IL.

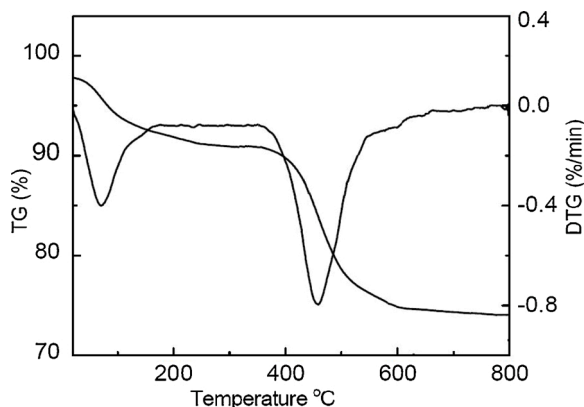


Fig. 5. Thermogravimetric analysis/differential thermogravimetric (TGA/DTG) curves for PMO-Py-IL.

2. Materials and methods

2.1. Material characterization

Textural properties of design nanomaterials were determined by using nitrogen physisorption measurements (77 K) using a Micromeritics ASAP 2000 instrument (Micromeritics, Norcross, GA, USA). Materials were degassed for 24 h at 100 °C under vacuum (10^{-4} mbar), prior to analysis. Surface area was calculated using the BET (Brunauer–Emmet–Teller) equation, while pore size distributions (D_{BJH}) and pore volumes (V_{BJH}) were worked out using the BJH method (Barrett, Joyner, and Halenda) from the N_2 adsorption branch.

Powder X-ray diffraction patterns were obtained in a Bruker-AXS diffractometer using $Cu\ K\alpha$ radiation ($\lambda = 1.5409\ \text{\AA}$). Low-angle X-ray diffractograms were recorded in the $0.5^\circ \leq 2\theta \leq 5^\circ$ range (step size 0.01° , 5 s time per step). Wide-angle diffraction patterns were collected in the $10^\circ \leq 2\theta \leq 80^\circ$ range at a scan time of 1.3 s (step size 0.017°).

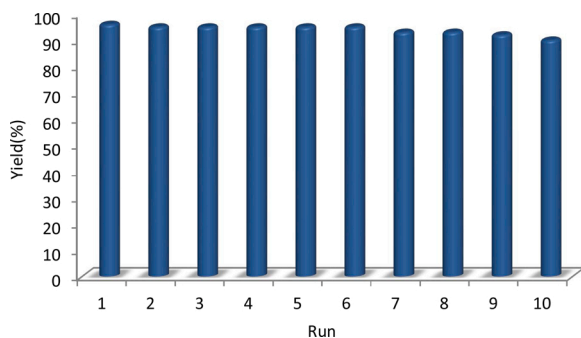


Fig. 6. Reusability of PMO-Py-IL nanocatalyst in the esterification of stearic acid and methanol.

Scanning electron microscopy (SEM) images were recorded in a Jeol JSM 6490 LA field emission apparatus, recorded at an acceleration voltage of 15 kV.

Thermogravimetric analysis (TGA) was performed from 25 to 800 °C using a heating rate of $10\ ^\circ\text{C}\cdot\text{min}^{-1}$ under static air atmosphere by a NETZSCH STA 409 PC/PG Instrument.

2.2. Synthesis of diethyl pyridine-2,6-dicarboxylate

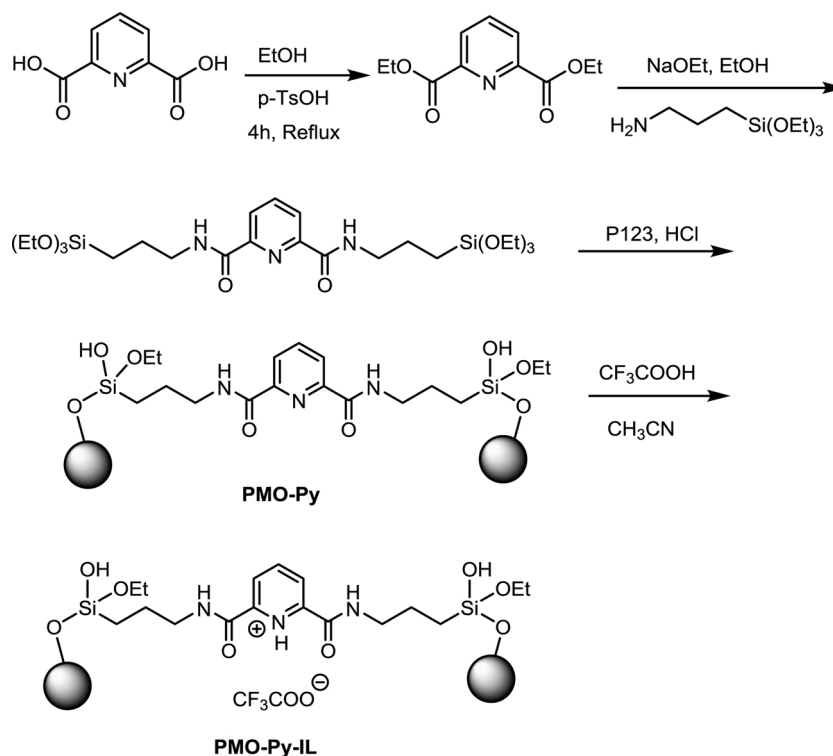
Diethyl pyridine-2, 6-dicarboxylate, employed as a bridging group, was prepared following a previously reported protocol [50]. Briefly, 50 mmol of pyridine-2,6-dicarboxylic acid and 1 mmol of *p*-toluenesulfonic acid (*p*-TsOH) in 100 mL ethanol were refluxed under stirring for 2 h, then diethyl pyridine-2,6-dicarboxylate was obtained after dissolving the solid residue obtained in about 30 mL of diethyl ether (subsequently washed with sodium bicarbonate solution and water), followed by drying (magnesium sulfate), filtration and solvent evaporation to yield pure diethyl pyridine-2,6-dicarboxylate as a white solid (95 % yield). ^1H NMR (300 MHz, CDCl_3): δ , 1.46 (t, $J = 8.7$ Hz, 6 H), 4.49 (q, $J = 8.7$ Hz, 4 H), 8.01 (t, $J = 8.5$ Hz, 1 H), 8.26 (d, $J = 8.4$ Hz, 2 H) ppm. ^{13}C NMR (75 MHz, CDCl_3): δ , 167.8, 149.6, 142.2, 131.0, 65.7, 15.7 ppm.

2.3. Synthesis of Bis(3-(Triethoxysilyl)Propyl)Pyridine-2,6-Dicarboxamide

Bis(3-(Triethoxysilyl)Propyl)Pyridine-2,6-Dicarboxamide was also obtained as previously reported [50] via heating at 170 °C (in a sealed tube under nitrogen atmosphere for 5 h) a mixture of sodium ethoxide (0.1 mmol), diethyl pyridine-2,6-dicarboxylate (10 mmol), and 3-(triethoxysilyl)propyl amine (20.5 mmol). Chloroform was added for extraction purposes and the final suspension was filtered (solvent removed under vacuum) to obtain pure bis(3-(triethoxysilyl)propyl)pyridine-2,6-dicarboxamide as a white solid (92 % yield). $\text{C}_{34}\text{H}_{67}\text{N}_3\text{O}_{11}\text{Si}_3$ (778.17): the calculated composition was C: 52.48, H: 8.68, N: 5.40, while the actual one was C: 53.01, H: 8.24, N: 5.14. ^1H NMR (300 MHz, CDCl_3): δ , 0.07 (m, 4 H), 1.16 (t, $J = 7.02$ Hz, 18 H), 1.72 (m, 4 H), 3.44 (m, 4 H), 3.72 (m, 12 H), 7.97 (d, $J = 8.4$ Hz, 1 H), 8.31 (d, $J = 8.4$ Hz, 2 H) ppm. ^{13}C NMR (75 MHz, CDCl_3): δ , 166.3, 151.5, 141.3, 127.1, 60.7, 44.4, 25.5, 20.6, 10.3 ppm.

2.4. Synthesis of PMO nanomaterials bearing pyridinedicarboxamide (PMO-Py)

Following our previously reported protocol [50], 12.5 g of 2 M HCl solution was employed to dissolve 0.4 g of Pluronic P123 (Aldrich, average $M_w \cong 5800$) under stirring at 35 °C, followed by the addition of 2.3 g of bis(3-(triethoxysilyl)propyl)pyridine-2,6-dicarboxamide, keeping the mixture under stirring for 20 h and subsequent aging (90 °C, overnight without stirring). The final material was filtered off and dried at 50 °C overnight, removing the template via solvent extraction in a solution of 1.0 mL 37 % HCl and 100 mL ethanol for 12 h. The



Scheme 1. Synthesis of protic pyridinium ionic liquid loaded periodic mesoporous nanomaterials (PMO-Py-IL).

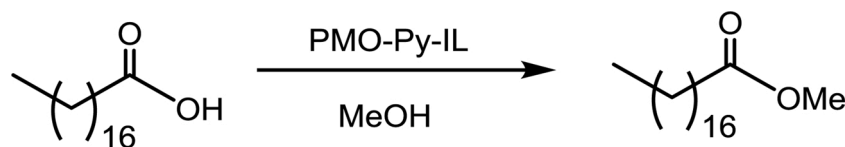
template-free material was eventually washed thoroughly with a mixture water/ethanol (24 h, Soxhlet apparatus) and dried at 80 °C overnight prior to its use. Finally, it was dried in an oven at 80 °C overnight.

2.5. Synthesis of PMO Materials bearing protic pyridinium ionic liquid (PMO-Py-IL)

2 g of PMO materials bearing Pyridinedicarboxamide (PMO-Py) were mixed with 10 mL of dry acetonitrile 3 mmol of trifluoroacetic acid were subsequently poured into the mixture under vigorous stirring for 5 h (at room temperature). The resulted protic pyridinium ionic liquid silica was filtered, washed with acetonitrile and dried under vacuum.

2.6. General procedure for biodiesel production using PMO-Py-IL materials

In a typical reaction, fatty acids (10 mmol), methanol or ethanol (5 mL), and PMO-Py-IL (0.1 g) as nanocatalyst were mixed in a 50 mL single-necked round bottomed flask and stirred under reflux conditions for 4 h. Upon reaction completion, the mixture was cooled down at RT, PMO-Py-IL was recovered and washed with ethyl acetate for the next run. The combined filtrate and ethyl acetate washings were washed with water and the organic layer was separated and dried over sodium sulfate, filtered, and concentrated under vacuum to provide the desired methyl esters as pure products.



Scheme 2. Esterification of stearic acid catalyzed by PMO-Py-IL.

3. Results and discussion

Novel PMO-Py materials were recently reported according to a two-step approach depicted in [Scheme 1](#). PMO-Py exhibited a high catalytic activity in the Knoevenagel condensation reaction [35]. Herein, the synthesis of an acidic hybrid organosilica with pyridinium ionic liquid framework as a solid-acid nanocatalyst is described. The synthesis of the pyridinium-based ionic liquid hybrid nanomaterial (PMO-Py-IL) was achieved by the addition of trifluoroacetic acid to PMO-Py. The obtained porous solid-acid pyridinium nanomaterial (PMO-Py-IL) was characterized by SEM, XRD, and nitrogen porosimetry analysis experiment.

3.1. Catalyst characterization

3.1.1. BET-BJH analysis

N₂ physisorption analysis of the organic-inorganic hybrid materials was performed to study their porosity. According to [Fig. 1](#), PMO-Py support and PMO-Py-IL nanocatalyst exhibited N₂-adsorption/desorption isotherms with hysteresis loop as IV type isotherm curves, classic of mesoporous materials. Hysteresis loop shape pointed to 2D hexagonal structures, so that the uniform dispersion of active trifluoroacetate exists within the pores of the material. As expected, after addition of trifluoroacetic acid and formation of pyridinium salt with trifluoroacetate counter ion, the average pore diameter and surface area of the modified materials (PMO-Py-IL) decreased ([Table 1](#)) ([Fig. 2](#)).

Table 2

Optimisation of reaction conditions in the esterification of stearic acid with methanol.

Entry	PMO-Py-IL (g)	Time (h)	T (°C)	Yield(%) ^b
1	–	10	reflux	10
2	0.2	6	reflux	96
3	0.1	6	reflux	95
4	0.1	3	reflux	90
5	0.1	4	reflux	95
6	0.05	4	reflux	72
7	–	10	reflux	70 ^c
8	0.1	6	45	55

^aAll reactions were carried out with 10 mmol of stearic acid and 5 mL of MeOH.^b Isolated yield.^c PMO-Py (0.2 mol%) was used as catalyst.

3.1.2. XRD analysis

Fig. 3 depicts low angle X-ray diffraction (XRD) patterns for PMO-Py materials, clearly showing a sharp signal corresponding to the (100) reflection and two additional less intense signals assigned to the (110) and (200) diffraction lines, suggesting a well-ordered 2D-hexagonal structure corresponding to the *P6mm* space group. By comparing the XRD data of PMO-Py-IL with PMO-Py, it was found that the diffraction peaks with lower intensity in PMO-Py-IL were observed at the same region and show no differences in XRD patterns. This evidence indicates that the ordered mesostructure is well preserved after trifluoroacetic

Table 3

Esterification of various fatty acids and alcohols catalyzed by PMO-Py-IL.

Entry	Substrate	Alcohol	Yield (%) ^a
1		MeOH	95
2		MeOH	95
3		MeOH	92
4		MeOH	92
5		Et OH	96
6		EtOH	96
7		MeOH	90
8		MeOH	92
9		MeOH	90

^a Isolated yield.

acid addition, with PMO-Py being stable under these conditions.

3.1.3. SEM analysis

Fig. 4 depicts scanning electron microscopy (SEM) images of PMO-Py-IL, consisting of uniform cylindrical/spheroidal shape structures as similarly reported for PMO-Py materials [50].

3.1.4. TG/DTG analysis

To assess the thermal stability of supported protic ionic liquid PMO-Py-IL thermogravimetric analysis/differential thermogravimetric analysis (TGA/DTGA) was performed (Fig. 5). TG and DTG curves displayed in Fig. 4 indicate three clear weight losses at different temperatures. A ca. 10 % mass loss could be observed up to 150 °C due to physisorbed water and ethanol (additional water loss via condensation of residual silanol and ethoxy groups). A further distinct weight loss (ca. 50 %) was found to be present in the 400–600 °C range, related to the removal of pyridinium moieties and remaining organics in the PMO structure. As-synthesized PMO-Py-IL materials exhibited a rather stable behavior towards temperature, keeping PMO-Py-IL framework thermal stability up to 400 °C.

3.2. Catalytic activity for the esterification of free fatty acids to produce biodiesel

After characterization of PMO-Py-IL, the esterification of stearic acid using different alcohols (methanol) was subsequently performed, with model reaction results shown in Scheme 2. Reaction parameters including quantity of catalyst, reaction temperature and times were

optimized (Table 2). Blank runs carried out without catalyst addition provided ca. 10 % of methyl stearate yield under reflux conditions in 10 h. Optimum conditions were achieved using 0.1 g PMO-Py-IL nanocatalyst under methanol reflux in 4 h (Table 2, entry 5) due to the high efficiency of the nanocatalyst. Compared to PMO-Py (Table 2, entry 7), higher product yield with less amount of catalyst was obtained by PMO-Py-IL which is attributed to the synergistic effect between pyridinium and trifluoroacetate ionic liquid in enhancing the activity of the catalyst.

To assess catalyst stability and leaching of active species from the support, a hot filtration test was conducted for the model reaction (esterification of stearic acid and methanol) under optimized conditions. The catalyst was removed via hot filtration after 1 h and the filtrate system proceeded to react for 5 h after catalyst removal. No esterification reaction progress was observed, pointing to the absence of any leached active species in the filtrate. These results confirmed strong incorporation and interaction of trifluoroacetate and pyridinium groups in the organosilica network not only could suppress leaching of active species, but also could enhance the catalytic activity of the catalyst via synergistic and cooperative effects.

These promising results were followed by detailed studies on substrate scope, using a broad range of renewable fatty acids (Table 3). As shown in Table 3, the isolated yields of esters ranged from 90 % to 96 % and the required time for the reaction completion was 4 h. Linear fatty acids such as palmitic, myristic, lauric, and stearic acid were reacted with methanol or ethanol to produce corresponding methyl or ethyl esters in high yields (Table 3, entries 1–6). Furthermore, this approach was amenable to the presence of other functionalities in the substrates such as carbonyl and alkene moieties, that remain completely unaffected for which biomass-derived substrates including oleic, levulinic and linoleic acid could be employed without any protection of their acid-sensitive functional groups under acid-catalyzed esterification reaction conditions (Table 3, entries 7–9). Most significantly, these excellent results provided strong evidence that the synergetic effects of pyridinium cation and trifluoroacetate anion in the mesoporous organosilica support were the key factors in catalyst performance to produce high yield of methyl esters under mild conditions.

In order to examine the viability of a robust and selective catalyst, the recyclability potential of PMO-Py-IL catalyst in the esterification between stearic acid and methanol was subsequently tested and evaluated under optimized conditions. Upon completion of the first formation of methyl stearate after 4 h, heterogeneous PMO-Py-IL was filtered off from the reaction mixture, washed with ethyl acetate and water followed by drying and reusing in the next run. PMO-Py-IL shows outstanding activity for at least ten additional runs under identical conditions to those of the fresh catalyst, preserving almost unchanged the original catalytic activity (Fig. 6).

4. Conclusions

Protic pyridinium based ionic liquid hybrid mesoporous materials (PMO-Py-IL) were successfully prepared by introduction of a 3-propyl triethoxysilane side chain to pyridine ring and formation of pyridine polysiloxane network followed by trifluoroacetic acid addition and subsequent ionic liquid organosilica formation. SEM, BET, TGA, and XRD patterns confirmed the interaction between the pyridinium cation and trifluoroacetate anion in the mesoporous material. After full characterization and structural confirmation, the resulted solid PMO-Py-IL could be utilized in esterification reaction between a broad range of free fatty acids and short chain alcohols. PMO-Py-IL hybrid materials showed the strong ability and activity toward the desired ester products and proved to be active and stable in the esterification reaction. Remarkably, an eco-friendly and feasible method for sustainable production of methyl esters has been accomplished using mesoporous supported protic ionic liquid with highly well-ordered surface area as a highly efficient and robust nanocatalyst.

Credit author statement

FATEMEH RAJABI

Experiments, funding, writing first draft

RAFAEL LUQUE

Revisions, discussion, writing final article and submission

Declaration of Competing Interest

The authors declare that they have no known competing financial interests or personal relationships that could have appeared to influence the work reported in this paper.

Acknowledgments

F. R. would like to acknowledge Payame Noor University and Iran National Science Foundation (INSF) for support of this work. The publication has been prepared with support from RUDN University Program 5-100.

References

- [1] P.S. Nigam, A. Singh, Production of liquid biofuels from renewable resources, *Prog. Energy Combust. Sci.* 37 (2011) 52–68, <https://doi.org/10.1016/j.pecs.2010.01.003>.
- [2] E.F. Aransiola, T.V. Ojumu, O.O. Oyekola, T.F. Madzimbamuto, D.I. O. Ikhuomogbe, A review of current technology for biodiesel production: state of the art, *Biomass Bioenerg.* 61 (2014) 276–297, <https://doi.org/10.1016/j.biombioe.2013.11.014>.
- [3] A.E. Atabani, A.S. Silitonga, I.A. Badruddin, T.M.I. Mahlia, H.H. Masjuki, S. Mekhilef, A comprehensive review on biodiesel as an alternative energy resource and its characteristics, *Renewable Sustainable Energy Rev.* 16 (2012) 2070–2093, <https://doi.org/10.1016/j.rser.2012.01.003>.
- [4] E.M. Shahid, J. Jamal, Production of biodiesel: a technical review, *Renewable Sustainable Energy Rev.* 15 (2011) 4732–4745, <https://doi.org/10.1016/j.rser.2011.07.079>.
- [5] B. Narowska, M. Kulazynski, M. Lukaszewicz, E. Burchacka, Use of activated carbons as catalyst supports for biodiesel production, *Renew. Energy* 135 (2019) 176–185, <https://doi.org/10.1016/j.renene.2018.11.006>.
- [6] A. Demirbas, *Biodiesel from Triglycerides via Transesterification*, Springer, 2008, pp. 121–140.
- [7] F. Ma, M.A. Hana, Biodiesel production: a review, *Bioresour. Technol.* 70 (1999) 1–15, [https://doi.org/10.1016/S0960-8524\(99\)00025-5](https://doi.org/10.1016/S0960-8524(99)00025-5).
- [8] I. Ambat, V. Srivastava, M. Sillanpää, Recent advancement in biodiesel production methodologies using various feedstocks: a review, *Renewable Sustainable Energy Rev.* 90 (2018) 356–369, <https://doi.org/10.1016/j.rser.2018.03.069>.
- [9] E. Fischer, A. Speier, Darstellung der Ester. *Ber. Dtsch. Chem. Ges. Chem. Eur.* 28 (1895) 3252–3258, <https://doi.org/10.1002/cber.189502803176>.
- [10] F. Cozzi, Immobilization of organic catalysts: when, why, and how, *Adv. Synth. Catal.* 348 (2006) 1367–1390, <https://doi.org/10.1002/adsc.200606096>.
- [11] X.S. Zhao, X.Y. Bao, W. Guo, F.Y. Lee, Immobilizing catalysts on porous materials, *Mater. Today* 9 (2006) 32–39, [https://doi.org/10.1016/S1369-7021\(06\)71388-8](https://doi.org/10.1016/S1369-7021(06)71388-8).
- [12] B.A.T. Mehrabadi, S. Eskandari, U. Khan, R.D. White, J.R. Regalbuto, A review of preparation methods for supported metal catalysts, *Adv. Catal.* 61 (2017) 1–35, <https://www.elsevier.com/books/advances-in-catalysis/song/978-0-12-812078-1>.
- [13] P. Munnik, P.E. de Jongh, K.P. de Jong, Recent developments in the synthesis of supported catalysts, *Chem. Rev.* 115 (2015) 6687–6718, <https://doi.org/10.1021/cr500486u>.
- [14] M. Kaur, S. Sharma, P.M.S. Bedi, Silica supported Brønsted acids as catalyst in organic transformations: a comprehensive review, *Chin. J. Catal.* 36 (2015) 520–549, [https://doi.org/10.1016/S1872-2067\(14\)60299-0](https://doi.org/10.1016/S1872-2067(14)60299-0).
- [15] A.E. Fernandes, A.M. Jonas, Design and engineering of multifunctional silica-supported cooperative catalysts, *Catal. Today* 334 (2019) 173–186, <https://doi.org/10.1016/j.cattod.2018.11.040>.
- [16] G.W. Huber, S. Iborra, A. Corma, Synthesis of transportation fuels from biomass: chemistry, catalysts, and engineering, *Chem. Rev.* 106 (2006) 4044–4098, <https://doi.org/10.1021/cr068360d>.
- [17] R. Rinaldi, F. Schüth, Design of solid catalysts for the conversion of biomass, *Energy Environ. Sci.* 2 (2009) 610–626, <https://doi.org/10.1039/B902668A>.
- [18] R. Gounder, Hydrophobic microporous and mesoporous oxides as Brønsted and Lewis acid catalysts for biomass conversion in liquid water, *Catal. Sci. Technol.* 4 (2014) 2877–2886, <https://doi.org/10.1039/C4CY00712C>.
- [19] V. Udayakumar, A. Pandurangan, Catalytic activity of mesoporous V/SBA-15 in the transesterification and esterification of fatty acids, *J. Porous. Mater.* 21 (2014) 921–931, <https://doi.org/10.1007/s10934-014-9839-y>.
- [20] Y. Wang, J. You, B. Liu, Preparation of mesoporous silica supported sulfonic acid and evaluation of the catalyst in esterification reactions, *Reac. Kinet. Mech. Cat.* 128 (2019) 493–505, <https://doi.org/10.1007/s11144-019-01645-2>.

- [21] S. Soltani, U. Rashid, S. Al-Resayes, I. Nehdi, Recent progress in synthesis and surface functionalization of mesoporous acidic heterogeneous catalysts for esterification of free fatty acid feedstocks: a review, *Energy Convers. Manage.* 141 (2017) 183–205, <https://doi.org/10.1016/j.enconman.2016.07.042>.
- [22] E.M. Björk, M.P. Militello, L.H. Tamborini, R.C. Rodriguez, G.A. Planes, D. F. Acevedo, M.S. Moreno, M. Odén, C.A. Barbero, Mesoporous silica and carbon based catalysts for esterification and biodiesel fabrication-The effect of matrix surface composition and porosity, *Appl. Catal. A Gen.* 533 (2017) 49–58, <https://doi.org/10.1016/j.apcata.2017.01.007>.
- [23] S.M. Silva, A.F. Peixoto, C. Freir, HSO₃-functionalized halloysite nanotubes: new acid catalysts for esterification of free fatty acid mixture as hybrid feedstock model for biodiesel production, *Appl. Catal. A Gen.* 568 (2018) 221–230, <https://doi.org/10.1016/j.apcata.2018.10.008>.
- [24] J. Gardy, E. Nourafkan, A. Osatiashiani, A.F. Lee, K. Wilson, A. Hassanpour, X. Lai, A core-shell SO₄/Mg-Al-Fe₃O₄ catalyst for biodiesel production, *Appl. Catal. B: Environ.* 259 (2019) 118093, <https://doi.org/10.1016/j.apcatb.2019.118093>.
- [25] W. Xie, F. Wan, Immobilization of polyoxometalate-based sulfonated ionic liquids on UiO-66-2COOH metal-organic frameworks for biodiesel production via one-pot transesterification-esterification of acidic vegetable oils, *Chem. Eng. J.* 365 (2019) 40–50, <https://doi.org/10.1016/j.cej.2019.02.016>.
- [26] M. Waki, Y. Maegawa, K. Hara, Y. Goto, S. Shirai, Y. Yamada, N. Mizoshita, T. Tani, W. Chun, S. Muratsugu, M. Tada, A. Fukuoka, S. Inagaki, A solid chelating Ligand: periodic mesoporous organosilica containing 2,2'-Bipyridine within the pore walls, *J. Am. Chem. Soc.* 136 (2014) 4003–4011, <https://doi.org/10.1021/ja4131609>.
- [27] Y. Chen, J. Shi, Chemistry of mesoporous organosilica in nanotechnology: molecularly organic-inorganic hybridization into frameworks, *Adv. Mater.* 28 (2016) 3235–3272, <https://doi.org/10.1002/adma.201505147>.
- [28] P. Van Der Voort, M.D. Esquivel Merino, E. De Canck, F. Goethals, I. Van Driessche, F.J. Romero-Salguero, Periodic mesoporous organosilicas: from simple to complex bridges; a comprehensive overview of functions, morphologies and applications, *Chem. Soc. Rev.* 42 (2013) 3913–3955, <https://doi.org/10.1039/c2cs35222b>.
- [29] O.V. Zenkina, *Nanomaterials Design for Sensing Applications*, Elsevier Inc., 2019.
- [30] R.S. Guimarães, C.F. Rodrigues, A.F. Moreira, I.J. Correia, Overview of stimuli-responsive mesoporous organosilica nanocarriers for drug delivery, *Pharmacol. Res.* 155 (2020) 104742, <https://doi.org/10.1016/j.phrs.2020.104742>.
- [31] O. Olkhovik, M. Jaroniec, Periodic mesoporous organosilica with large heterocyclic bridging groups, *J. Am. Chem. Soc.* 127 (2005) 60–61, <https://doi.org/10.1021/ja043941a>.
- [32] A. Douhal, M. Anpo, *Chemistry of Silica and Zeolite-based Materials*, Elsevier Inc., 2019, pp. 1–25.
- [33] J.G. Croissant, X. Cattoën, M.W. Chi Man, J.-O. Durand, N.M. Khashab, Syntheses and applications of periodic mesoporous organosilica nanoparticles, *Nanoscale* 7 (2015) 20318–20334, <https://doi.org/10.1039/C5NR05649G>.
- [34] J.C. Manayil, A.F. Lee, K. Wilson, Functionalized periodic mesoporous organosilicas: tunable hydrophobic solid acids for biomass conversion, *Molecules* 24 (2019) 239, <https://doi.org/10.3390/molecules24020239>.
- [35] V.I. Pärulescu, C. Hardacre, Catalysis in ionic liquids, *Chem. Rev.* 107 (2007) 2615–2665, <https://doi.org/10.1021/cr050948h>.
- [36] T. Welton, Room-temperature ionic liquids. Solvents for synthesis and catalysis, *Chem. Rev.* 99 (1999) 2071–2084, <https://doi.org/10.1021/cr980032t>.
- [37] N.V. Plechkova, K.R. Seddon, Applications of ionic liquids in the chemical industry, *Chem. Soc. Rev.* 37 (2008) 123–150, <https://doi.org/10.1039/B006677J>.
- [38] C. Dai, J. Zhang, C. Huang, Z. Lei, Ionic liquids in selective oxidation: catalysts and solvents, *Chem. Rev.* 117 (2017) 6929–6983, <https://doi.org/10.1021/acs.chemrev.7b00030>.
- [39] T.L. Greaves, C.J. Drummond, Protic ionic liquids: evolving structure–property relationships and expanding applications, *Chem. Rev.* 115 (2015) 11379–11448, <https://doi.org/10.1021/acs.chemrev.5b00158>.
- [40] G. Cai, S. Yang, Q. Zhou, L. Liu, X. Lu, J. Xu, S. Zhang, Physicochemical properties of various 2-hydroxyethylammonium sulfonate-based protic ionic liquids and their potential application in hydrodeoxygenation, *Front. Chem.* 7 (2019) 196, <https://doi.org/10.3389/fchem.2019.00196>.
- [41] H. Luo, H. Yin, R. Wang, W. Fan, G. Nan, Caprolactam-based Brønsted acidic ionic liquids for biodiesel production from Jatropha oil, *Catalysts* 7 (2017) 102, <https://doi.org/10.3390/catal7040102>.
- [42] M. Hoque, M.L. Thomas, M.S. Miran, M. Akiyama, M. Marium, K. Ueno, K. Dokko, M. Watanabe, Key factor governing the physicochemical properties and extent of proton transfer in protic ionic liquids: ΔpK_a or chemical structure? *RSC Adv.* 8 (2018) 9790–9794, <https://doi.org/10.1039/C8CP06973E>.
- [43] P.P. Mohire, D.R. Chandam, R.B. Patil, D.R. Kumbhar, S.J. Jadhav, A.A. Patravale, V.P. Godase, J.S. Ghosh, M.B. Deshmukh, Protic ionic liquid promoted one pot synthesis of 2-amino-4-(phenyl)-7-methyl-5-oxo-4H, 5H-pyran[4,3-b]pyran-3-carbonitrile derivatives in water and their antimycobacterial activity, *J. Heterocycl. Chem.* 55 (2018) 1010–1023, <https://doi.org/10.1002/jhet.3133>.
- [44] I. Cota, F. Medina, R. Gonzalez-Olmos, M. Iglesias, Alanine-supported protic ionic liquids as efficient catalysts for aldol condensation reactions, *C. R. Chimie* 17 (2014) 18–22, <https://doi.org/10.1016/j.crci.2013.06.004>.
- [45] X. Zhang, D. Su, L. Xiao, W. Wu, Immobilized protic ionic liquids: efficient catalysts for CO₂ fixation with epoxides, *J. CO₂ Util.* 17 (2017) 37–42, <https://doi.org/10.1016/j.jcou.2016.11.005>.
- [46] R. Izumi, Y. Yao, T. Tsuda, T. Torimoto, S. Kuwabata, Pt-nanoparticle-supported carbon electrocatalysts functionalized with a protic ionic liquid and organic salt, *Adv. Mater. Interfaces* 5 (2018) 1701123, <https://doi.org/10.1002/admi.201701123>.
- [47] A. Ilyas, N. Muhammad, M.A. Gilani, K. Ayub, I.F.J. Vankelecom, A.L. Khan, Supported protic ionic liquid membrane based on 3-(trimethoxysilyl) propan-1-aminium acetate for the highly selective separation of CO₂, *J. Membran Sci.* 543 (2017) 301–309, <https://doi.org/10.1016/j.memsci.2017.08.071>.
- [48] M. Abdollahi-Alibeik, M. Pouriaeyvali, Nanosized MCM-41 supported protic ionic liquid as an efficient novel catalytic system for Friedlander synthesis of quinolones, *Catal. Commun.* 22 (2012) 13–18, <https://doi.org/10.1016/j.catcom.2012.02.004>.
- [49] H. Zhang, H. Li, H. Pan, A. Wang, S. Souzanch, C. Xu, S. Yang, Magnetically recyclable acidic polymeric ionic liquids decorated with hydrophobic regulators as highly efficient and stable catalysts for biodiesel production, *Appl. Energy* 223 (2018) 416–429, <https://doi.org/10.1016/j.apenergy.2018.04.061>.
- [50] R. Luque, J.C. Colmenares, *An Introduction to Green Chemistry Methods*, Future Science Ltd, London, 2013.
- [51] F. Rajabi, A. Zare Ebrahimi, A. Rabiee, A. Pineda, R. Luque, Synthesis and characterization of novel pyridine periodic mesoporous organosilicas and its catalytic activity in the Knoevenagel condensation reaction, *Materials* 13 (2020) 1097, <https://doi.org/10.3390/ma13051097>.
- [52] F. Rajabi, F. Fayyaz, R. Bandyopadhyay, F. Ivars-Barcelo, A.R. Puente-Santiago, R. Luque, Cytosine palladium hybrid complex immobilized on SBA-15 as efficient heterogeneous catalyst for the aqueous Suzuki-Miyaura coupling, *Chem. Select* 3 (2018) 6102–6106, <https://doi.org/10.1002/slct.201800348>.
- [53] F. Rajabi, F. Fayyaz, R. Luque, Cytosine-functionalized SBA-15 mesoporous nanomaterials: synthesis, characterization and catalytic applications, *Microporous Mesoporous Mater.* 253 (2017) 64–70, <https://doi.org/10.1016/j.micromeso.2017.06.043>.